

Double-Slit Interferometry: The De Broglie Particle-Wave Duality



Jacques Rault*

Solid State Physics Laboratory, Paris-Sud University, France

Submitted: July 31, 2023; Published: August 21, 2023

*Corresponding author: Jacques Rault, Solid State Physics Laboratory, Paris-Sud University, France Email: jacques.rault@yahoo.fr

Abstract

The de Broglie wavelength $\lambda = h/mv$ of simple particles (photon, electron, neutron) atoms (helium, neon) and molecules (fullerene, fluorine porphyrin) deduced from the de Broglie (dB) relation and those measured by double slits interferometry are compared. The de Broglie relation is verified in very large domains of velocity v and mass m of the particles, respectively 8 and 13 orders of magnitude. In this paper one analyses the interference spectra of photons and electrons and give the Intensity Relations IR(II-DI) between the interference intensity (II) by two slits and the diffracted intensity (DI) by one slit. The double slits interference in the de Broglie-Bohm interpretation is an interference of particle and pilot waves, internal and external waves each passing by a different slit. The velocities of these waves are discussed. From the universal de Broglie relation and the relation $v_p = v_w$ between the particle and pilot waves one shows that only in the domain of the maximum of the light spectrum ($\lambda_m \sim 550 \mu\text{m}$) the dB relation leads to the Plank-Einstein (PE) relation $h\nu = mc^2$. A measure of the mass of the photon $m^* = 4 \cdot 10^{-36} \text{ Kg}$ is deduced. The de Broglie relation for different wave lengths shows that the PE relation must be modified, the velocity of light is not constant as shown by various experiments: Global Positioning Systems GPS, red shift in astronomy etc. This has been discussed by Marmet in years 2000. The same conclusion was given by Sato in 2010 for electromagnetic waves. The trajectories of electrons observed by Jönsson by double slits interferometry and then calculated by Gondran according to the de Broglie-Bohm interpretation are then analyzed in detail. The correlations observed between the properties of these trajectories at short and long distances from the slits permit to give the general equation of the trajectories. The origin of these properties is discussed in the framework model of De Broglie and Bohm, assuming that at any point the intensity of the two waves (particle and pilot wave) passing by the 2 slits are decreasing functions of the distance to the slits. The changes of direction of the trajectories are explained.

Keywords: Neutrons; Fluorine Porphyrin; Photon; Velocity

Introduction

Young's double-slit interferometry (DSI) [1] is the most used technique for verifying the De Broglie [2] & Bohm [3] interpretation of the wave-particle duality, see for example the books of Cohen-Tanoudji et al. [4] & Feynman [5], this last author considered that this type of experiment has in it the heart of quantum mechanics. These experiments have been realized with photons electrons neutrons atoms and mesoscopic single objects such as fullerenes C60 and C70 and Fluorine Porphyrin, see references in the review of Gondran et al. [6,7] & of Nairz et al. [8]. In all these experiments, for most authors the path of the quantum particles cannot be determined, this would be a consequence of the uncertainty or indistinguishability principles. Only recently some authors [9] have been able to follow the trajectories of the photon in DSI and in the Mac-Zehnder interferometer (MZI) and found that self-interference (SI) fringes of coherent single photon are exactly the same as that of the classical interference

(CI) of coherent photons ensemble of a laser; Kim and Ham [10] concluded that "the classical coherence ... is rooted by the single photon self-interferences". DSI of electrons have been studied by Jönsson [11] in 1961 and then by several authors, see references [6,7]. Crease [12] published this experiment under the title "The most beautiful experiment in Physics World 2002". Tonomura et al. [13] gave a demonstration of single electron build up (electrons one by one) of an interference pattern.

The aim of this paper is:

- to give the relation between the de Broglie and Plank-Einstein relations which leads to a measure of the mass of the photon.
- to study in detail the DSI trajectories of electrons calculated by Gondran et al.

Correlations between the behaviour at short and long distances from the slits are pointed out. From these properties, never noted up to now, the equations of the trajectories are deduced, the origin of the various changes of orientation of these trajectories due to quantic superposition [14] is then discussed.

The de Broglie (dB) relation

The de Broglie wavelength of particles

It is important to compare the wave-particle duality of small and large particles which have been studied by different authors.

The mass of photons is not known or assumed to be negligible and that of other particles are well known and can be experimentally varied. This comparison permits us to give an estimate of the speed and the mass of the photons. One gives below the experimental conditions of these authors: the mass m of the particles the velocity V and the wave lengths λ deduced from the de Broglie relation $\lambda = h/mV$ ($h = 6.6 \cdot 10^{-34}$ Js) measured by interferometry. According to the authors these two wavelengths (electrons and large particles) are not different. For the very different types of particles, one compares in table 1 the parameters (m, V, λ) obtained in different experimental DSI conditions.

Table 1: De Broglie wavelength λ of particles of mass m and velocity v observed by DSI at room temperature. λ of the sun corresponds to the maximum of the emission spectrum.

	v m/s	m (Kg)	λ
Photon (sun)	$3 \cdot 10^8$	$4 \cdot 10^{-36}$	550 nm
Electron	$1.8 \cdot 10^8$	$9.1 \cdot 10^{-31}$	4.9 pm
Neutron	2200	$1.6 \cdot 10^{-27}$	0.18 nm
Helium	960 at 83 K 1780 at 295 K	$6.6 \cdot 10^{-27}$ " "	1.03 \AA 0.56 \AA
Neon	1.25	$3.3 \cdot 10^{-26}$	16 nm
Fullerene C ₆₀	120	$1.2 \cdot 10^{-24}$	4.6 pm
	200	" "	2.8
	220	" "	2.5
F. Porphyrin L12	85	$1.7 \cdot 10^{-23}$	500 fm

Photon

This mass is really unknown, various authors between 1873 and 1971 gave some limiting superior values m^* between 10^{-39} to 10^{-48} g using different terrestrial and extra-terrestrial methods, see references in the reviews of Vasseur [15] and Tu et al. [16]. Often one finds in the textbooks that m^* is negligible. The intensity spectrum of the light (sun and galaxies) is well known [17]. A large maximum intensity is observed for $500 < \lambda \text{ nm} < 600$ in the yellow region. Assuming that the reported velocity of the light c ($\approx 3 \cdot 10^8$ m/s) has been measured in this region the de Broglie relation leads to: $3.67 < m^* \cdot 10^{36} \text{ Kg} < 4.4$ then to $m^* = 4 \cdot 10^{-36}$ Kg for the $\lambda = 550$ nm corresponding to the maximum intensity of the spectrum.

Electron

Jönsson [11] gave the trajectories of electrons of velocity $v = 1.8 \cdot 10^8$ m/s in a two slits interferometer, see also figures 1 & 2 in the review of Gondran et al. [7]. The mass of the electron being $9.1 \cdot 10^{-31}$ Kg, the de Broglie length is $\lambda = 4 \cdot 10^{-12}$ m, From the peak's interferences reported in figure of ref. [7] one deduced the wavelength: $\lambda = 4.9 \cdot 10^{-12}$ m.

Neutron

The interferences of a beam of neutrons ($m = 1.67 \cdot 10^{-27}$ Kg) of velocity $v = 2200$ m/s are analyzed in the book of Rauch & Werner [18]: the de Broglie length is 0.18 nm.

Helium

Carnac & Mlynek [19] used the classical two slits interferometer to analyze the interferences of Helium $m = M/Na = 6.6 \cdot 10^{-27}$ g ($m = 4$ uma, Na Avogadro number). An intense atomic beam is obtained by a supersonic gas expansion and by changing the temperature of the reservoir, the mean velocity of the atoms and therefore the De Broglie wavelength is adjusted; at $T_1 = 295$ K $\lambda_1 = 0.56$ and at $T_2 = 83$ K $\lambda_2 = 1.03$ A. These values are in very good agreement with the observed values deduced from the interference's peaks on the detector screen. From the relations $\lambda = h/mv$ and $kT \sim mv^2$ one verifies the relation $\lambda_1/\lambda_2 = v_2/v_1 = (T_2/T_1)^{1/2} = 0.53$.

Neon

Shimizu et al. [20] using a vertical two slits interferometer have studied the effect of gravity on the interference fringes for different initial velocities $0 < v < 2$ m/s and transit times. For $v = 1.25$ m/s and $m = 3.3 \cdot 10^{-26}$ Kg, $\lambda = 16$ nm in agreement with the extrapolated value deduced from their figures 3 & 4.

Fullerene

The mass of C₆₀ is $1.2 \cdot 10^{-24}$ Kg, Arndt et al. [21] gave the interference pattern produced by these molecules having velocities of 120 200 and 220 m/s (see for example their figure 2a). The experimental de Broglie lengths deduced from the interferences are respectively $\lambda = 2.5$ 2.8 and 4.6 pm in total agreement with the

de Broglie relation. From the first peak of the interference pattern (one finds exactly the same de Broglie length.

Fluorous Porphyrin

Eibenberger et al. [22] utilized the Kapitza-Dirac-Talbot-Lau interferometer (KGTLI) for analyzing the interferences of large particles of FP (C₄ H₁₉₀ F₃₂₀ N₄ S₁₂). The mass of these organic particles having 810 atoms (mass M=10123 amu) is m=M/Na = 1.7 10⁻²⁰ g and the velocity v = 85 m/s, the De Broglie length is λ= 4.5 fm. The authors found a good agreement between the measured

mass and the mass deduced from the de Broglie relation.

The experimental de Broglie lengths of these 7 particles are given in table 1 the wave lengths of all particles (10 data) verify the dB relation:

$$\lambda_{dB} = h / mv \quad ; \quad \log \lambda_{dB} = \log h - \log(mv) = -33.18 - \log(mv) \quad (1)$$

with h = 6.62 10⁻³⁴ (Js), m (kg), λ (m), the correlation coefficient is Rc = 0.995. The same relation is verified for helium and fullerene with constant mass but with different velocities.

Table 2: The fit parameters Xc and mi (in au) for these two trajectories for curves I3 and I6.

	Xc	m1	m2	m4	Rc
I3	4.2	0.047	-0.014	0.244	0.9945
I6	4.5	0.032	0.042	0.585	0.9955

Assuming that the velocity c = 299 782 458 10⁸ m/s ~ 3 10⁸ m/s of the light has been measured in the domain of the maximum intensity of the spectrum (yellow, λ= 550 nm) one deduces the mass of the photon m* = 4 10⁻³⁶ Kg, this is the most direct and simple method to measure this mass. Up to now there is no other method to measure the mass of the photon. There is a huge literature on the upper limit values of this mass m_{sup}, (m_{sup} ≈ 10⁻⁴³ to 10⁻⁵⁰ kg), the authors using different experimental methods, see the reviews of Vasseur [23] and Tu et al. [24]. These authors concluded that “Up to now there has been no conclusive evidence of a finite mass of the photon”.

Two important remarks must be given:

a) The comparison between electron (relativistic v = 0.6 c) and fullerene (non-relativistic v = 4 10⁻⁶ c) is interesting, these two particles of different nature have a mass ratio m(el)/m(fu) = 7.5 10⁻⁸ but same ratios mv(ful)/mv(el) = 1.65 and λ(el)/λ (ful) = 1.6. This property indicates clearly that the de Broglie waves, called internal and external waves (or particle and pilot waves) do not depend on the charge of the particle but only on the impulsion mv value.

b) Photons and electrons (Jönsson experiments) are relativistic particles; the velocities are higher than 10% the velocity c of light. It is well known that the relativist relation giving the wavelength as function of the observer velocity v_{obs} gives the classical Doppler relation for v_{obs} < c / 10.

Relation between the de Broglie and the Planck-Einstein relations

The wave-particle duality

De Broglie has assumed that the pilot wave passes by the two slits and interferes. In complex waves which present a group velocity vg and a phase velocity v_φ the relation v_g v_φ = c² (c: light

velocity) is generally used [23], this relation obviously is not valid for monochromatic waves and also in non-dispersive medium. De Broglie used a similar relation v_p v_w = c² between the velocities v_p of the particle and v_w of the wave. The wavelength λ = V_w / ν given by the de Broglie relation λ= h / m v_p leads to the Planck-Einstein relation:

$$hv = mc^2. \quad v_p \quad v_w = c^2 \quad (1)$$

these two relations have never been discussed, but nevertheless accepted because in total agreement with the Einstein hypothesis: the constant velocity of light.

In fact, has noted by Marmet [24,25] many phenomena (red shift in astronomy, Global Positioning Systems (GPS) Galileo and others positioning technologies) prove that the experimental velocity of light with respect to an observer moving at velocity v in same or opposite direction is c ± v. Sato [26] observed that the velocity of electromagnetic waves is dependent on the observer velocity. In 1997 Marmet concluded that “this apparent constant velocity of light with respect to a moving frame is the most fascinating illusion in science”.

In fact, the interference patterns (DSI and MZI) of light and electrons (see hereafter) show that v_p = v_w, then the wavelength λ= v_p / ν is given by the de Broglie relation λ = h / m v_p:

$$hv = mv_p^2, \quad v_p = v_w \quad (2)$$

For photons in the yellow region (λ~ 550nm) the measured velocity of light is v_p = c then the Planck-Einstein relation is obtained. The wave particle duality relation v_p = v_w and the de Broglie relation explain the interference properties of photons and massive particles of different dB wave lengths. The assumption, v_p v_w = c² (never verified), made by de Broglie in 1927 for obtaining the Einstein relation is then wrong and must be replaced by the relation v_p = v_w observed by DSI and MZI.

Self-interference (SI) fringes of electrons

Gondran et al. [7] presented in 2014 a numerical simulation of the double slit experiments of electrons performed by Jönsson [11] in 1961 which demonstrated the continuity between classical and quantum mechanics. The method of Feynman Path Integrals (FPI) is used to calculate the de Broglie-Bohm waves functions. The trajectories of electrons in DSI experiments, obtained by Gondran et al (figure 5 of ref. [7]) are given in figures 1 & 2, the velocity of the electrons is $v = 1.3 \cdot 10^8$ m/s, the distance between

slits is $d = 0.8 \mu\text{m}$ and between slits and screen $D = 10$ or 35 cm, the width of the horizontal slits is $a = 0.2 \mu\text{m}$. The electron mass is $m = 9.1 \cdot 10^{-31}$ Kg then the de Broglie wavelength is $\lambda = 4 \cdot 10^{-12}$ m. From the interference peaks a similar wavelength, $\lambda = 5.3 \cdot 10^{-12}$ m, is measured. In figure 1 one gives the classical method for determining λ , the blue line OM_1 is the axis between the origin of the DSI and the first intensity peak on the screen. The orthogonal projection of OSu on OM_1 in red is $\Delta L/2 = \lambda/2$, ΔL being the difference of length between the axis parallel to OM_1 passing by Su and SL .

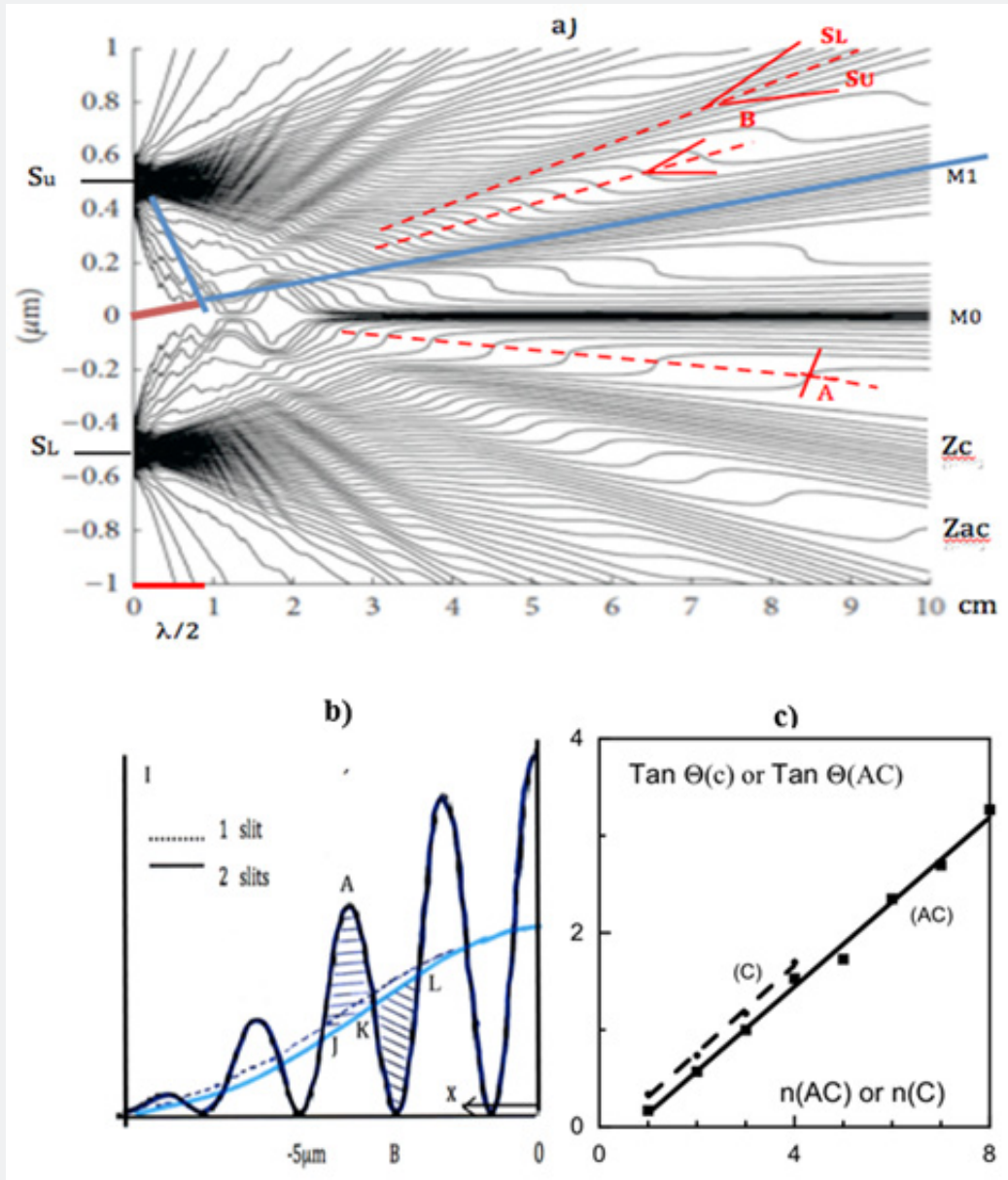


Figure 1: a) Double slits Interferometry: trajectories of electrons in the Su and SL domains according to the Gondran model see figure of [7] Definition of the correlation Z_c and anti-correlation Z_{ac} zones. The axis OM_1 is the direction of the first intensity peak. b) Intensity spectrum on the screen at distance $D= 35$ cm of the slits. The blue line is obtained by rotation $-\pi$ the area KAI around K to obtain the area KBL (and so on). The dashed black line is the intensity curve obtained by simple diffraction by one slit. c) Tangents $\Theta(c)$ and $\Theta(ac)$ of the M_i and AC_i axis as function of the numbering index $n(C)$ and $n(AC)$, Θ is in degree (au) deduced from figure a.

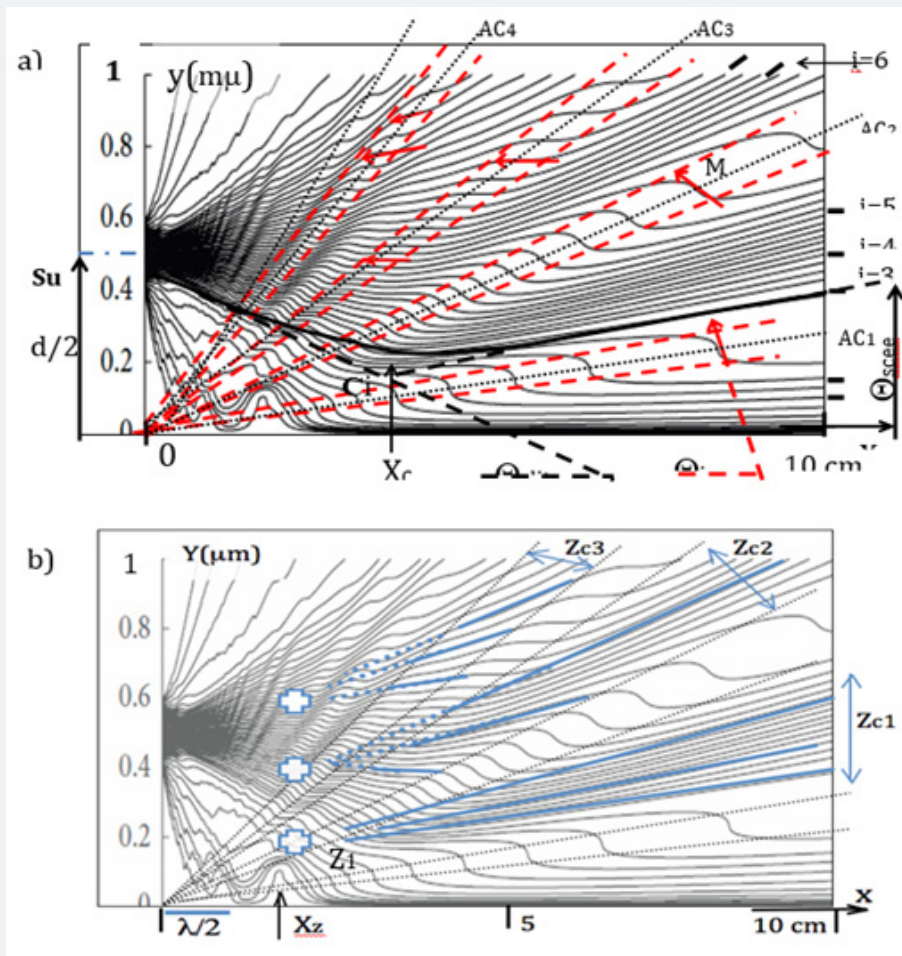


Figure 2: a) Electron trajectories in the S_u domain, Gondran model from ref. 7. The correlation Z_c and anti-correlation Z_{ac} domains are separated by dashed red lines. AC_i dashed black lines are the direction of minimum intensity of the intensity spectrum on the screen. Red arrows are the tangent to the trajectory jump in the Z_{ac} domains. The black heavy line is the I_3 curve, the tangents near the screen and the slits, cross at point $C_i (X_c, Y_c)$.
 b) Fan structure of the tangents to the trajectories for $X > X_z$ in the different domains Z_{ci} . Large hollow crosses Z_i : convergent zones of the tangents at long distance.

For simplicity all angles θ and lengths given here are deduced from the figure of ref. [6] and are given in arbitrary unit (au): θ in degree y in μm and x in cm. The relation between $\tan \theta$ au and its value $\tan \theta$ rs in the real space rs is $\tan \theta$ rs = $1.56 \cdot 10^{-5} \tan \theta$ au. In figure 1b one gives the intensity spectra obtained on the screen at the distance $D = 35$ cm from the slits, reproduced from figure 4d of ref. [7], heavy line is the DSI interferences intensity (II), dashed line is the diffraction intensity (DI) by one slit only obtained in the same experimental conditions.

One verifies that the total intensities III and IDI, area below the curves II and DI of figure 1b in the domain $-10 \mu m < x < 0$ are equal. In the figure one has defined the points J K L, the crossing points of the II and DI lines. It is important to note that the ordinates of these points are equal to the half values of the intensity interference peak ($AK=KB$). In the figure it is shown that the two hatched areas

are equal, the curve KBL by rotation π around K is superposed to the curve KAJ, the next intensity peaks verify this property. In DSI all electrons missing in the non-coherent domain are in fact found in the coherent (adjoining) domain. The relations between the total and partial peak intensities:

$$I_{\Pi} = I_{DI} \quad \text{and} \quad I_{KBL} = I_{KAJ} \quad I_{R(\Pi - DI)} \quad (3)$$

never noted up to now are called the Intensity Relations of the II and DI phenomena $IR(II-DI)$. It must be noted that when the screen is very near the slits ($D=3.5$ cm, see figure 4c of ref. [7]) the interference diagram is more complex, but the same relation is observed. The principal properties deduced from these figures are

- a) no trajectory crossing the symmetry plane OM_0 .
- b) the relation between the intensity curves II and DI.

c) the relation between the area of the different correlation and anti-correlation parts (KAJ and KBL) of a same intensity DI curve.

These properties are clear evidence that the system of interferences obtained by DSI is in fact a single-electron buildup of an interference pattern.

Relation between the wavelength deduced from DSI and by diffraction

By diffraction by only one slit of width a, the intensity is given in figure 1b (dashed black curve). The diffracted intensity [5] at

distance x on the screen is $I(x) / x = I_0 \sin^2(X) / X^2$, $X = x \pi a / \lambda D$ which go to zero at $x_{dif} = \lambda D/a$, this value must be compared to x_{int} the distance of the first interference peak $x_{int} = \lambda D/d$. From figure 1b one concludes that the wave lengths deduced by the two processes are very similar: 4.9 pm (diffraction) and 4.4 pm (interference). In figure 1c one verifies that for electrons the ratio $x_{dif} / x_{int} = d/a = 4$ is the number of interference peaks in the domain of diffraction $\theta < x_{dif} / D$. This property also observed for monochromatic light and Neon (figure 3 of ref. [18]) has never been noted.

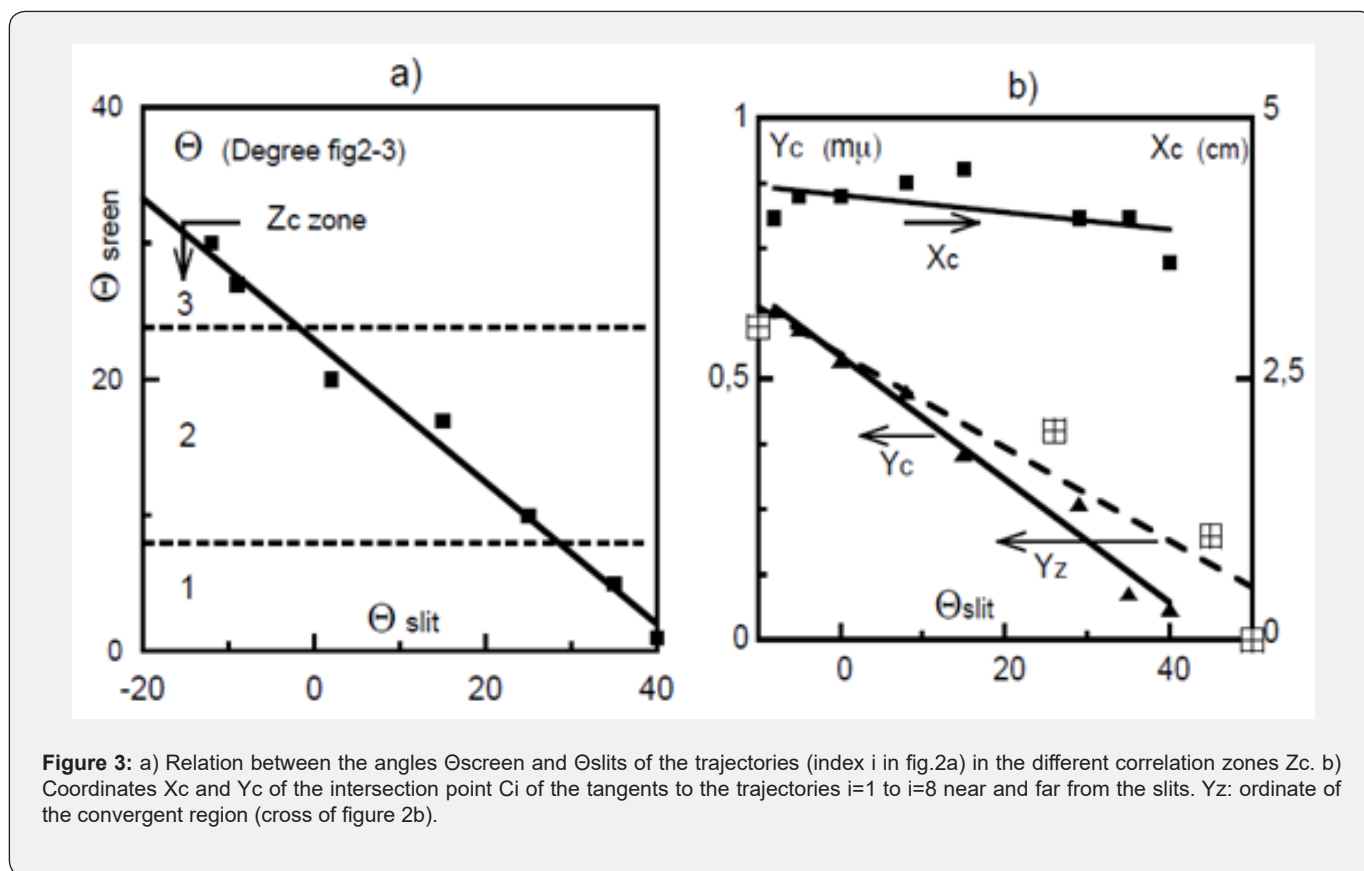


Figure 3: a) Relation between the angles Θ_{screen} and Θ_{slits} of the trajectories (index i in fig.2a) in the different correlation zones Z_c . b) Coordinates X_c and Y_c of the intersection point C_i of the tangents to the trajectories $i=1$ to $i=8$ near and far from the slits. Y_z : ordinate of the convergent region (cross of figure 2b).

Relation between the Direction of Maximum and Minimum Intensity

In figures 2a & 2b the domains of correlation Z_{ci} and anti-correlation Z_{aci} are defined (heavy dashed red lines in fig a, black dotted lines in figure b), i is the numbering $n(c)$ or $n(ac)$ of the two types of domains, these domains correspond to those observed in figure 1b giving the intensity on the screen (or detector). It is important to note that from figure 2a the minimum intensity on the screen can be deduced from the lines AC_i passing by the inflexion points of each trajectory and by the symmetry centre of

the double slit.

The angles θ_c and θ_{ac} directions of maximum and minimum intensity are measured (in degree, arbitrary unit) from the Gondran et al figures. In figure 1c are reported $\tan \theta_c$ (4 points deduced from the interference diagram of figure 1b) and $\tan \theta_{ac}$ (8 points deduced from the dotted lines in figure 2a) as function of the numbering $n(C)$ and $n(AC)$ of the domains. The dashed line deduced from the DSI is the classic result: $\tan \theta_c = n(C) \lambda / d$, $n(C)$ is generally called the order of the fringe. The plain line is the linear fit of $\tan \theta_{ac}$ versus $n(ac)$, the correlation factor is excellent $R_c = 0.997$. The slopes of $\tan \theta_{ac}$ and $\tan \theta_c$ are equal. The shift Δn

=1/2 to superpose the two curves is obviously due to the fact that the abscissa of the first minimum intensity is the half value of that of the adjacent maximum one as shown in figure 1b.

In conclusion the Broglie wavelength λ can be deduced from the slope of $\tan \theta_{ac}$ either at long distance D near the screen or

a short distance near the slits (in the domain $2.5X_c$ and 10cm of figure 2 in arbitrary units, see below). Generally, λ is deduced from the maximum of the first interference peak at long distance slits-screen D, figure 2 shows that λ can be deduced with accuracy from the first minimum at short distance.

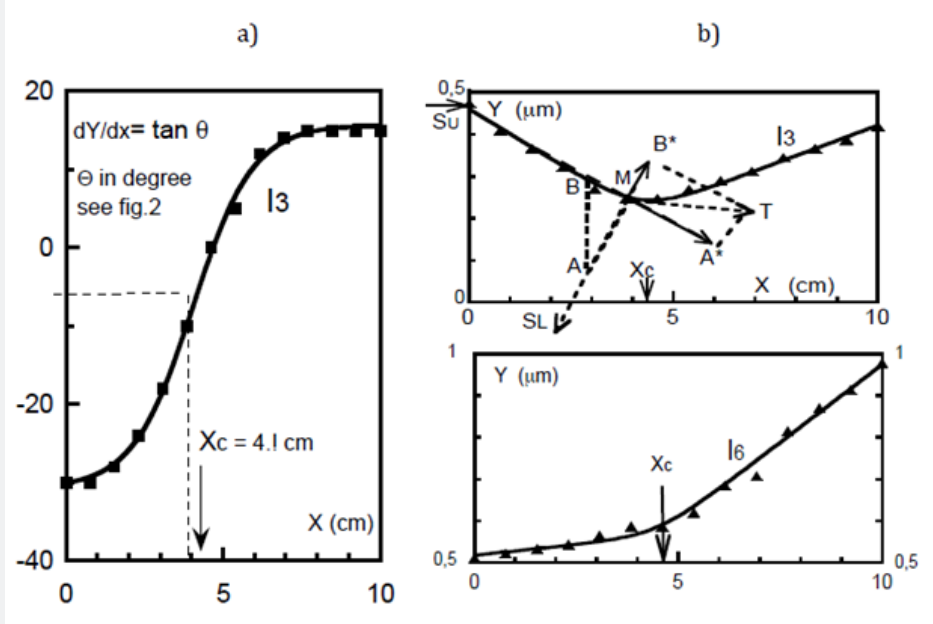


Figure 4: a) Squares: slope, $\tan \Theta$ values, of the I3 curve as function of the distance x , the curve is the fit with relation (7), X_c is the coordinate of the minimum of the intensity $y(x)$ and intersection of the tangents near and far from the slits (figure 2a).

Relation between the Direction of the Trajectories at Short and Long-distance D

In figure 3a the relation between the angles θ_{scr} and θ_{slit} of the trajectories measured near the screen and the slits is given. θ_{scr} (in au) is deduced from figure 2, 8 curves have been selected (index i and marked by small heavy mark near the screen). The θ_{slit} data are deduced from figure of ref. [7] enlarged and by extrapolation in the domain $0 < x < 2$ cm. The linear relations in the diagram of figure 2 (degree, au) and in the real space (rs):

$$\theta_{scr} = 25 - 0.5576\theta_{slit} \quad (au, \text{deg ree}) \quad (4a)$$

$$\theta_{scr} = 8.4 \cdot 10^{-6} - 0.7\theta_{slit} \quad (rs, -3 \cdot 10^{-6} < \theta_{slit} < 1.2 \cdot 10^{-5}) \quad (4b)$$

are observed. The correlation factor is $R_c = 0.988$. the uncertainty comes essentially from the θ_{slit} measurements. In the figure the different zones Z_{ci} are indicated.

In conclusion whatever is the correlation zone Z_{ci} the above correlation rule between the trajectory angles at low and long distances is observed.

Change of Direction of a Single Trajectory

In figure 2a the trajectory $i = 3$ in heavy line is shown as an example, the different linear behaviours at short and long

distances is a general property of all trajectories. The change of orientation occurs at the coordinates (X_c, Y_c) , the intersection points C_i of the tangents. These coordinates for the 8 curves ($1 < i < 8$) of figure 2 are given in figure 3b as function of θ_{slit} . Y_c is a linear relation of θ_{slit} and X_c is quasi constant:

$$Y_c = 0.548 - 9 \cdot 10^{-3} \theta_{slit} \quad (au, \mu m) \quad R_c = 0.944 ; 4 < X_c < 4.6 \quad (au, cm) \quad R_c = 0.55 \quad (5)$$

As shown in the figure X_c can be approximated by a linear function of θ_{slit} (straight line) but the correlation factor is very bad, $R_c = 0.55$. In figure 2a the half wavelength $\lambda/2$ determined in figure 1 is represented in blue on the abscise in arbitrary unit, one concludes that: $X_c = 2 \lambda = 3.7$ cm (au). In real space $X_c = 11 \cdot 10^{-12}$ m (rs).

Fan Structure of the Trajectories at Long Distance in the Z_c domains

In figure 2b in each domain Z_c the tangents to 3 trajectories are indicated in blue. In each domain the extrapolated tangents from the slits converge to the same restricted region of average coordinates $X_z Y_z$. The convergent point of the fan structure is represented by large crosses. For the three domains Z_{ci} the value X_z is constant, independent on the numbering i , $X_z = \lambda = 1.8$ cm in (au). The ordinate is a linear function of the numbering i of the

zone Z_{ci} : $Y_z = i \cdot 0.2 \mu\text{m}$. In figure 3b the values of Y_z and Y_c are compared. One concludes that these two parameters verify the relations:

$$X_c = 2X_z = 2\lambda = 3.7\text{cm (au)} = 11 \cdot 10^{-12} \text{ m (rs)}; Y_c \sim Y_z \quad (6a)$$

Calling $\theta(Z_i)$ and $\theta(M_i)$ the angles of the directions OZ_i of the convergence points Z_i and of the directions OM_i of the intensity peaks M_i (i order of the fringe), from figure 2b & figure 1b one verifies the relation in the real space:

$$\tan \Theta(Z_i) = 2 \tan \Theta(M_i) = 12i \cdot 10^{-6} \text{ (rs)} \quad (6b)$$

which again precise the correlations between the trajectories at short (2 cm) and long (35 cm) distances from the slits. In conclusion in the Gondran diagrams the wavelength λ generally deduced from the interferences at long distance (peaks M_i) can be deduced from the convergence point Z_i at low distance from the slits.

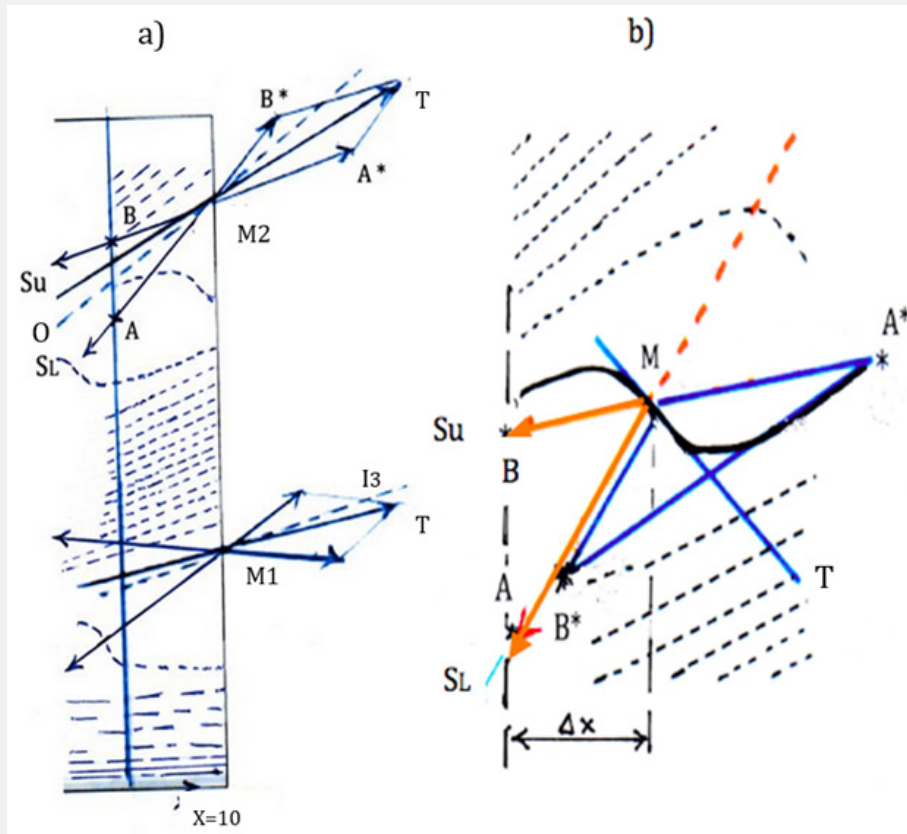


Figure 5: a) Border of the figure 2a. Dashed lines are the trajectories. At two points M_1 and M_2 the directions of the slits MSu and MSL are given. The graphical method, see text, leads to tangents MT nearly parallel to the trajectories. b) Enlarged domain around point M of figure 2a. M is on the AC_2 axis. The directions of the slits MB and MA are indicated. The points A^* and B^* are deduced from relation (9). The tangent MT deduced from the graphical model is exactly tangent to the jump of the trajectory (heavy black line) in the anti-correlation domain.

Equation of the Trajectories as Function of the Slits-Screen Distance

As example in figure 4a the slope $dy/dx = \tan \theta$ of trajectory $i = 3$ of figure 2 is plotted as function of the distance x from the slits. The slopes are constant near and far from the slits and a nonlinear variation with θ (slit) is observed in a small region around X_c . This is the typical variation of the function $y = \tanh x$ then the data are fitted with the tanh function:

$$dy / dx = -7.7 + m_1 * \tanh(m_2(x - m_3)) ; m_1 = 23.2 ; m_2 = 0.525 ; m_3 = 4.1 \text{ (au)} \quad (7)$$

m_i are the fit parameters in (au). The slope at $x = m_3 = 4 \text{ cm}$ is -7.7 degrees, this is the $(\theta_{\text{screen}} - \theta_{\text{slit}}) / 2$ value as shown in figure 4a. The value found $m_3 = 4.1 \text{ (au)}$ is about the value $X_c = 3.7 \text{ cm (au)}$ and $X_c = 4 \text{ cm (au)}$ determined in figure 2 by the intersection of the tangents at $x = 0$ and $x = 10 \text{ cm}$ and by the minimum of $y(x)$. The correlation factor R_c of the fit with these parameters is excellent: $R_c = 0.9994$. As the primitive of $\tanh x$ is

$\ln(\cosh(x))$ [27] one has reported in figure 4b the trajectories $y(x)$, $i = 3$ and 6, deduced from the relation:

$$y(x) = m4 + m2 * (x - Xc) + m1 * \ln(\cosh(x - Xc)); \quad 4.2 < Xc < 4.5 \quad (au) \quad (8)$$

The correlations factors R_c is excellent. The value of X_c determined from relations 5, 6 are not very different from the measurements deduced from the trajectories of figures 2 & 3.

Origin of the Change of Direction of the Trajectories

A somewhat analogy of waves interactions in water and in DSI near the slits and at long distance have been pointed out by Scarini [28], Couder et Fort. [29] showed that small drops of liquid (millimetre size) in DSI experiment present interferences figure very analogous to that of photons or electrons; at long distances the orientation of the trajectory depends on the orientation of the two waves and on their amplitudes at the meeting point. These effects in liquid have been discussed by Bush [30].

In simple diffraction of electrons by one slit S_u (Figure1b) the intensity at a point M on the screen is a decreasing function of distance x on the screen and on the distance screen -slits D; one assumes then that the intensity of the wave coming from slit S_u (or S_L) is inversely proportional to the length MS_u (or MS_L). This assumption permits to give a simple geometrical method for determining the direction of the tangents to the trajectories at short and long distance from the slits in the Z_{Ci} and AC_i domains.

Correlation zone (Z_{Ci})

At X_c the trajectories directions change drastically. Figure 5a shows the direction changes observed on trajectories I3 and I6. In the figure the trajectory I3 is analyzed in detail. At a point M near the X_c point, minimum of $y(x)$, the waves directions S_{uM} and S_{LM} are given. These lines intersect the arbitrary vertical (dashed) line at $x = 3\text{cm}$ (au) at points B and A; the segments MA and MB are proportional to the distances to the slits S_L and S_u . From these points A and B one defines the points A^* and B^* on MB and MA: the segments MA^* and MB^* (intensity of the two waves) are parallel to the slits direction S_u and S_L , and verify the relations: $MA^* = MA$ and $MB^* = MB$. The intensities are then:

$$MA^* = k / MS_u, \quad MB^* = k / MS_L; \quad MA^* = k' / MS_L, \quad MB^* = k' / MS_u \quad (9)$$

In the second expression $k' = k / MS_u MS_L$. We are only interested in orientation and relative values. In the figure the resulting vector is then obtained, and one verifies that this vector is the tangent to the trajectory I3 at point M. In figure 5a the same property is observed for the I6 trajectory. In figure 5a one has applied the same procedure to the points M1 and M2 at distance $x=10\text{ cm}$ from the slits (Figure 2a) M1 and M2 are near the I3 and I6 trajectories. One remarks that the calculated direction MT is nearly parallel to the trajectory (dashed line). The above model of waves interaction leads to a MiT direction nearly tangent to the trajectories in the Z_c domains.

Anti correlation zone (AC_i)

In figure 5b the enlarged zone of point M of figure 2a ($x = 7.8\text{ cm}$, $y = 0.6\text{ }\mu\text{m}$) is represented. This point is on the anti-correlation line AC_2 (dashed line). The direction of the slits S_L and S_U are indicated in yellow. The vectors MA^* and MB^* (in blue) are proportional to the intensity of the waves coming from the slit directions MB (S_u) and MA (S_L). As the phases of these waves are opposite at the centre of this AC zone the resulting direction is plotted. There is an excellent agreement between the direction of the trajectory at the inflexion point (jumps in the anti-correlation domain) and the MT direction deduced from the above model of wave interactions.

In conclusion the proposed model of wave interactions and the model of Gondran et al would explain the direction of the trajectories at short and long distance from the double slits and the important changes of direction in the intermediary domains.

Conclusion

The de Broglie relation is verified in very large domains of velocity and mass of the particles, respectively 8 and 13 orders of magnitude. The Plank-Einstein relation, assuming that the velocity of light is constant, has never been verified. For photons at the maximum of the intensity spectrum of the sun light ($\lambda = 550\text{ nm}$) this relation (rel.2) is deduced from the de Broglie relation noting that the particle and pilot waves have same velocity. From these relations the mass of the photon is found $m^* = 4 \cdot 10^{-36}\text{ Kg}$. As noted by various authors there is an excellent agreement between the mass of heavy particles determined by different methods and the De Broglie relation. It is important to find others experimental methods which permit us to measure accurately the photon mass.

We have analyzed the properties of the electron trajectories deduced by Gondran et al from De Broglie and Bohm interpretation and the FPI method without invoking the principles of indistinguishability and indeterminism. The double slit interference of electrons is in fact an interference of waves, generally called internal and external waves (or particle and pilot waves); electrons passing by the slit S_u (or S_L) do not cross the symmetry plane. It has been shown that the total intensities of DSI and diffraction by one slit are equal. Also, the different parts (correlation and anti-correlation) of an interference diagram are equal, the IR(II-ID) rel.3 summaries these properties.

All trajectories passing by a slit S_u (or S_L) present the same properties:

- a) trajectories are linear near and far from the slits, there is a constant linear relation between these directions of each trajectory, rel.4.
- b) an important change of direction at a constant characteristic distance X_c from the slits.

c) a fan structure of the tangents to the trajectories at long distances ($x > X_c$), the convergence point at X_z is independent of the correlation zone, the relation between X_c X_z and the wave length λ has been given (rel.6a,b, figure 3).

d) From these properties the equations of the trajectories and their slopes are deduced (rel.7,8), these simple relations fit with a great accuracy the calculated trajectories of Gondran et al.

e) finally, a geometrical process of interaction of the De Broglie et Bohm waves have been proposed to explain the origin of the change of direction of the trajectories in the correlation and anti-correlation domains. Interferences of other types of particles should be studied similarly to verify the properties of the De Broglie et Bohm waves "the earth of the quantum mechanics".

References

1. T Young (1807) Lectures on Natural Philosophy, 464 Johnson, London, UK.
2. Broglie DL (1927) Wave mechanics and the atomic structure of matter and radiation. *J Phys et le Radium*, 8(5): 225-241.
3. Bohm D (1952) A Suggested Interpretation of the Quantum Theory in Terms of Hidden Variables. *I Phys Rev* 85: 166.
4. Cohen CT, Diu B, Laloe F (1977) Quantum Mechanics. John Wiley et Sons, New York, USA.
5. Feynman R (1989) Lectures on Physics Addison. Wesley, Boston, USA.
6. Gondran M, Gondran A (2005) Numerical simulation of the double slit interference with ultracold atoms. *Am J Phys* 73(6): 507-515.
7. Gondran M, Gondran A (2014) Measurement in the de Broglie-Bohm Interpretation: Double-Slit, Stern-Gerlach, and EPR-B. *Phys Res Inter*.
8. Nairz O, Arndt M, Zeilinger A (2003) Quantum interference experiments with large molecules. *Am J Phys* 71(4): 319-325.
9. Kocsis S, Braverman B, Ravets S, Stevens MJ, Mirin RP (2011) Observing the average trajectories of single photons in a two-slit interferometer. *Science* 332(6034): 1170-1173.
10. Kim S, Ham BS (2021) Revisiting self-interference in young double-slit experiments. arXiv: 2104.08007.
11. Jönsson C (1961) Electron interference at several artificially produced fine gaps. *Magazine for physics* 161: 454-474.
12. Crease RP (2002) *Physics World* September 1.
13. Tonomura A, Endo J, Matsuda T, Kawasaki T, Ezawa H (1989) Demonstration of single-electron buildup of an interference pattern. *American Journal of Physics* 57: 117-120.
14. Zeilinger (2010) *Dance of the photons*, Edit. Farrat, Strauss, Giroux.
15. Vasseur G (1996) Limits on the photon mass CEA-DAPNIA/SPP 96-07.
16. Tu LC, Luo J, Gillies GT (2005) The mass of the photon. *Rep Prog Phys* 68(1): 77.
17. Roussel L (1972) *Forest Photology*, Masson.
18. Rauch H, Werner SA (2015) *Neutron Interferometry: Lessons in Experimental Quantum Mechanics, Wave-Particle Duality, and Entanglement*. Oxford University Press, USA, 12.
19. Carnac O, Mlynek J (1991) Young's double-slit experiment with atoms: A simple atom interferometer. *Phys Rev Letters* 66(21): 2689.
20. Shimizu F, Shimizu K, Takuma H (1992) Double-slit interference with ultracold metastable neon atoms. *Phys Rev A* 46(1): R17.
21. Arndt M, Nairz O, Andreae JV, Keller C, Zouw GVD, et al. (1999) Wave-particle duality of C60 molecules. *Nature* 401(6754): 680-682.
22. Eibenberger S, Gerlich S, Arndt M, Mayor M, Tüxen J (2013) Matter-wave interference of particles selected from a molecular library with masses exceeding 10000 amu. *Physical Chemistry Chemical Physics* 15(35): 14696-14700.
23. Lochak G (1962) *CR Acad Sc* 254: 4436.
24. Marmet P (1997) *Einstein's theory of relativity versus classical mechanics* Gloucester Ontario Canada: Newton Physics Books, 2401.
25. Marmet P (2000) The GPS and the Constant Velocity of Light. *Acta Scientiarum, Universidade Estadual de Maringá, Brazil*, 22(5): 1969-1279.
26. M Sato (2010) The velocity of electromagnetic wave is observed differently depending on the observer's velocity. *Physics Essays* 23(3): 405.
27. <https://fr.wikipedia.org/wiki/Tangente-hyperbolique>
28. Scarani V (2004) *Initiation a la Physique Quantique*, Vuibert, Paris.
29. Couder Y, Fort E (2006) Single-Particle Diffraction and Interference at a Macroscopic Scale. *Phys Rev Letters* 97(15): 154101.
30. Bush JWM (2015) *Pilot-Wave Hydrodynamics*. *Annual Rev Fluid Mechanics* 47: 269-292.



This work is licensed under Creative Commons Attribution 4.0 License
DOI: [10.19080/JOJMS.2023.08.5557289](https://doi.org/10.19080/JOJMS.2023.08.5557289)

Your next submission with JuniperPublishers will reach you the below assets

- Quality Editorial service
- Swift Peer Review
- Reprints availability
- E-prints Service
- Manuscript Podcast for convenient understanding
- Global attainment for your research
- Manuscript accessibility in different formats
(Pdf, E-pub, Full Text, Audio)
- Unceasing customer service

Track the below URL for one-step submission

<https://juniperpublishers.com/submit-manuscript.php>